Formation of USJ with cluster implants for 32nm node and beyond

Karuppanan Sekar and Wade Krull

SemEquip Inc.
34 Sullivan Rd, North Billerica, MA-01862, USA
Phone: +1-978-262-9500 E-mail: ksekar@semequip.com

Abstract

Cluster Ion implantation is an attractive alternative approach to realize applications in semiconductor devices at 32nm node and beyond. Cluster ions have a special property of making self-amorphous layer even at a lower dose. Here we will discuss the self-amorphizing properties of heavier cluster ion species like B_{36}, B_{18} and C_{16} and discuss how these could be substituted for various implants in devices like low energy SDE, PAI and co-implant applications. For applications with ultra-low energy requirements below 500eV, B_{36} species can provide both process and throughput advantage without any device related issues due to energy contamination.

1. Introduction

Ion implantation is a standard and precise technique to place dopants at a desired depth at a given dopant concentration in semiconductor device fabrication. As gate lengths are reduced, the vertical and lateral dimensions of the doped regions in the source and the drain must be reduced as well to achieve and maintain adequate device electrical characteristics. With shrinking gate length and scaling constraints, the ion implantation energy used to fabricate these devices should be scaled down to sub keV regime to meet ultra-shallow junction depth (Xj) requirements. Conventional implantation methods for p-type dopants using B and BF_2 suffer from lower throughput at very low energies due to the limitation imposed by the space charge effect at very low implantation energies. Ultra-shallow junction (USJ) depth requirements also place rigid conditions on the avoidance of channeling phenomenon which is severe at ultra low energies. Cluster ion implantation [1-3] is an attractive alternative approach to resolve and counter these issues (i.e., high throughput and reduced space charge effect). Large concentrations of defects are created after every implant and the dopants are electrically inactive. To provide electrically active dopant concentration with no implant generated defects one needs to perform post implant thermal annealing. Thermal annealing leads to boron TED effects and boron clustering. Dissolution of the boron clusters require high temperature anneal producing the issue of deeper junction depth due to boron diffusion. As a trade-off between activation and diffusion, high temperature short anneals (millisecond anneal) have been developed. Usage of co-implants (such as C, F etc) is another approach that provides boron diffusion control [4,5].

The use of a pre-amorphizing implant (PAI) (either Ge or Xe) produces a high dopant activation with a low thermal budget and therefore with minimal diffusion [6,7]. However, PAI implants produce EOR damage that is difficult to anneal, creating leaky devices. Cluster Ion implantation provides an opportunity to address all of the above mentioned issues (in 32nm nodes and beyond) experienced in the semiconductor device fabrication. Cluster Boron species ($B_{18}H_{22}$) (hereafter referred as B_{18}) and dimer $B_{18}H_{22}$ i.e., $(B_{18}H_{22})_2$ (hereafter referred as B_{36}) provide useful process advantages for fabrication of USJ junctions. Cluster Carbon species $C_{16}H_{10}$ (hereafter referred as C_{16}), C_7H_7 (hereafter referred as C_7) are used as co-implants for boron diffusion control.

Advantages of B_{18} over monomer boron and BF_2 studies have been discussed in our earlier publications [8]. In this article we will highlight self-amorphization and discuss the amorphous layer thicknesses produced by the various cluster ion species B_{18}, B_{36}, C_{16} & C_7 and discuss their effect on the activation behavior of the dopants. We will show examples that demonstrate the effect of using carbon cluster ions as boron diffusion control implants. Finally we will demonstrate the crystal quality of the damaged implanted region upon thermal annealing. The

978-1-4244-3320-9/09/$25.00 ©2009 IEEE

advantages of using cluster ion species to counter the existing issues with very low energy implants will be presented.

2. Experiment

All of the wafers used in this study were 200mm, n-type, (100) silicon substrates. The wafers were implanted with boron & carbon at different energies and doses using $B_{18}H_{22}$ & $C_{16}H_{10}$ materials from a ClusterIon® source. The sequence of implant is: Cluster Carbon implants first, then Cluster Boron implant. $C_{16}H_{10}$ implant energy is 2keV & 3keV per carbon atom at a dose of 1e15. $B_{18}H_{22}$ and dimer $B_{18}H_{22}$ implants (B_{36})were done at various energies 300 to 500eV per boron atom at an equivalent dose of 1e15 atoms/cm^2.

The anneals in this work were performed on the Mattson Technology Canada flash anneal system using impulse Flash Assist RTP or fRTP [9] and also using Excico Laser Anneal System. Sheet resistance measurements were carried out using a four-point probe. Dopant Profiles were measured with Secondary Ion Mass Spectrometry (SIMS) and 5e18 atoms/cm^3 level defined as Xj and XTEM measurements were carried out using commercially available facilities.

3. Results and Discussions

Since the amorphous layer is critical in achieving very shallow, abrupt and highly activated junctions, we have studied the self-amorphization feature of cluster implants in detail.

(a) Amorphous layer thickness

Fig. 1 shows XTEM images B_{18} and B_{36} species at an implant energy of 300eV per boron atom @ dose 1e15 atoms/cm^2. The amorphous layer thickness in the case of B_{18} [Fig. 1(a)] is around 4.7-5.0nm. In the case of B_{36} [Fig. 1(b)] is around 5.9-6.3nm. The amorphous layer thickness with B_{36} implant is 20-25% higher than the case with B_{18}. To achieve the amorphous layer thickness equivalent to B_{36} either one needs to increase the dose or the energy of B_{18}. Incidentally the amorphous layer thickness for 500eV per boron atom implant with B_{18} yielded ~ 6.2nm @ dose 1e15 atoms/cm^2 (Fig. 2) .

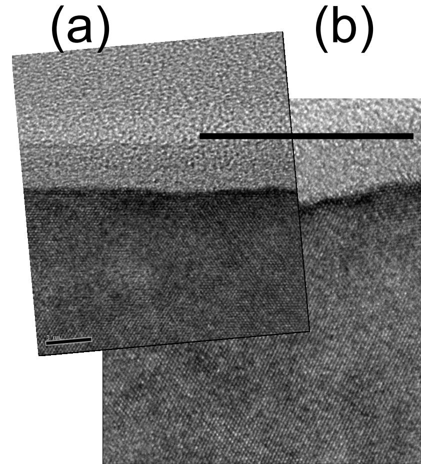

Fig. 1 shows XTEM images of B_{18} and B_{36} species implanted at 300eV per boron atom @1e15 atoms/cm^2. The amorphous layer thickness in the case of B_{18} ~4.8-5.0nm and for B_{36} ~ 6.3nm.

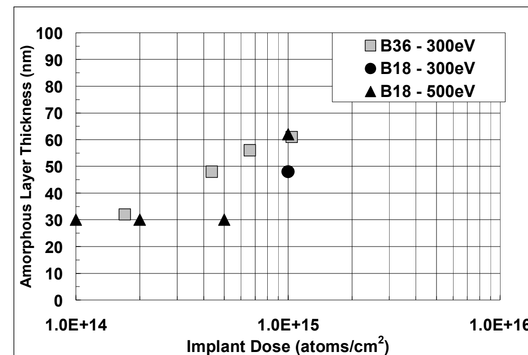

Fig. 2 shows amorphous layer thickness at various doses for B_{18} @ 500eV per atom and B_{36} @ 300eV per atom implant energies. For comparison the amorphous layer thickness (~ 4.8nm) for B_{18} @ 300eV per atom at 1e15 atoms/cm^2 is also shown

Fig. 2 shows the comparison of amorphous layer thickness for B_{18} and B_{36} at 500eV and 300eV respectively per boron atom implant energy at various doses. In the case of B_{18} and at 500eV per boron atom energy, the onset of amorphization starts (XTEM pictures not shown here) around 2e14 atoms/cm^2 but the continuous amorphous layer formation begins after a dose of 5e14 atoms/cm^2. But for B_{36} case and even at lower energy, at 300eV per boron atom energy, the onset of amorphization starts below 2e14

atoms/cm^2 but the continuous amorphous layer formation begins after a dose of 3e14 atoms/cm^2. The above analyses show that with heavier cluster species B_{36}, one can achieve higher amorphous layer thickness than B_{18}. for a given energy and dose. Also the threshold dose for amorphization is also lower with heavier cluster species like B_{36}. Later we will show how this feature is relevant in getting better activated layers.

(b) Cluster ions as co-implant species

As we all know that co-implants have been successfully utilized in controlling boron diffusion and getting enhanced activation. It has been shown earlier that use of C_{16} to control boron diffusion and obtain an abrupt junction with 500eV per atom implant energy [10]. For 32nm technology node and beyond the junction depth requirements are such that Xj < 10 – 12 nm are required. To get to these numbers one needs to go lower implant energies with no diffusion or minimal diffusion anneal technologies. This eliminate the option for spike anneals in most cases and the place is taken over by millisecond anneal (flash anneal or laser anneal) where junction movement less than 2nm could be achieved. Now the question arises whether co-implant species are of any use in these advanced technologies. As we already know that an amorphous layer enhances dopant activation and avoids channeling, it is then important to understand and study cluster carbon species where they can provide some process advantages owing to their self-amorphizing property. By choosing suitable energy and dose of the cluster carbon species, we can utilize those implants as a PAI-implant and could be used as a diffusion control too. Presence of carbon could lead to higher sheet resistance numbers and so it becomes important to make a trade off between amorphous layer thickness and Rs requirements. Fig. 3 shows amorphous layer thicknesses for C_{16} implant at various energies (1 to 5keV per carbon atom) for a dose of 1e15 atoms/cm^2. The amorphous layer thickness varied from a low 50Å to high 400Å. Depending on the requirement for a device fabrication one can tune in the amorphous layer thickness by choosing the energy and dose of the cluster carbon species and as an added benefit it provides an abrupt dopant profile too.

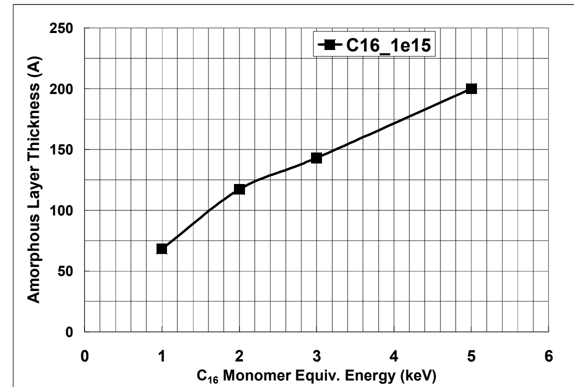

Fig. 3 shows amorphous layer thickness at various energies (1 to 5keV per atom implant energy) for C_{16} @ 1e15 atoms/cm^2 .

(c) Dopant Profile Analysis

For PMOS source-drain extension (SDE) implants higher concentration of boron in the range of 1e21 atoms/cm^3 are required to be placed within a smaller depth region. Junction depth as low as 10nm are expected to be typical for 32nm and beyond technology nodes. As mentioned earlier, one has to make a trade off between activation and diffusion if one wants to get high activation numbers using high temperature fast annealing. In amorphous Si, the nucleation of B clusters depends on the B concentration. If the B concentration is lower than 10^{20} cm^{-3}, all B atoms are incorporated into substitutional positions during the regrowth of the amorphous layer [11]. It is important to verify how the boron activation behaves with self-amorphizing cluster boron implants. First one has to start with a boron profile with Xj less than 10nm. Fig. 4 shows a high depth resolution (HDR) and PCOR protocol boron SIMS profile for 300eV per atom for B_{18} and B_{36} implants. The Xj @ 5e18 atoms/cm^3 for B_{18} profiles are 7.8nm & 10.2nm for HDR and PCOR protocols. There is a difference of about 2.4nm difference in Xj between these two SIMS protocols along with a better abruptness with HDR protocol. Using a millisecond anneals and allowing a diffusion of 2nm, one can achieve Xj around 10nm just with B_{18} species. If we look at the B_{36} profile, Xj ~ 11.8nm with PCOR protocol. With HDR protocol, in the case of B_{36} the expected Xj is around 9.4nm. The channeling tail is buried in the case of PCOR protocol whereas it is very evident with HDR protocol. The channeling tail starts around 1e18 atoms/cm^3 boron concentration at about a depth of 8nm. By

suitably utilizing the self-amorphizing property of a cluster-carbon co-implant, the channeling tail can be eliminated.

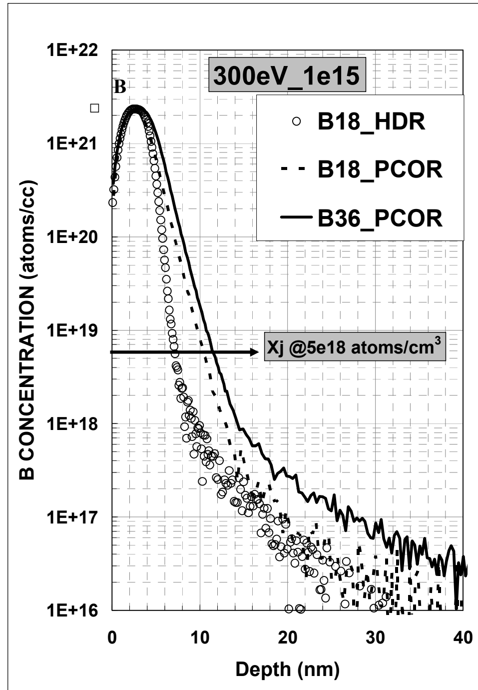

Fig. 4 shows a high depth resolution (HDR) and PCOR protocol boron SIMS profile for 300eV per atom for B_{18} and B_{36} implants. The Xj @ 5e18 atoms/cm^3 for B_{18} profiles are 7.8nm & 10.2nm for HDR and PCOR protocols.

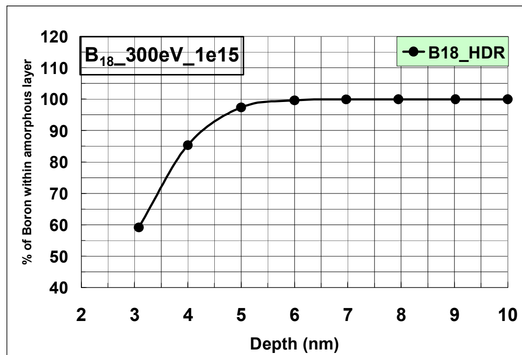

Fig. 5 shows the cumulative percentage of boron at different depths for B_{18} 300eV per boron atom energy at a dose of 1e15 atoms/cm^2. More than 50% of the dopants lie in the top 3nm.

Let us go over to the detailed analysis of a HDR SIMS profile for B_{36} . Fig. 5 shows the cumulative percentage of boron at different depths for 300eV per boron atom energy at a dose of 1e15 atoms/cm^2. At a depth around 5.5nm, almost 100% of boron concentration is enclosed within. If an amorphous layer thickness of around 6nm is created by the cluster boron implant almost the entire boron concentration is within the amorphous layer which will aid in dopant activation. Thus B_{36} will provide better junction depth, abruptness and activation when compared to other species.

Fig. 6 shows the SIMS profile for B_{36} at 300eV per atom implant energy at various doses. We can see that the SIMS profile moves deeper with increasing dose. To obtain a certain Xj, one can either choose energy or dose with certain restrictions. Depending on the device conditions with various screen oxide thicknesses one can select the suitable energy and dose.

(d) Activation

. Fig. 6 shows Rs and Xj data for 300eV per atom implant energy for B_{18} with cluster carbon co-implants. The implant energy per atom for C16 species are 2keV and 3keV at a dose of 1e15 atoms/cm^2.

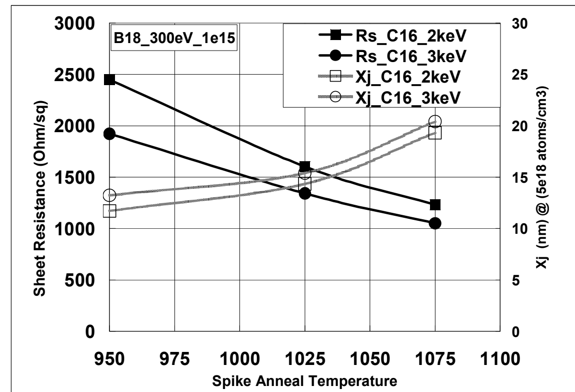

Fig. 6 shows Rs and Xj data for 300eV per atom implant energy for B_{18} with cluster carbon co-implants. The implant energy per atom for C16 species are 2keV and 3keV at a dose of 1e15 atoms/cm^2. The Rs values are smaller with 3keV per atom implant energy than 2keV. Xj values close to 12nm could be achieved with low temp spike anneal.

The Rs values are smaller with 3keV per atom implant energy than 2keV. Xj values close to 12nm could be achieved with low temp spike anneal. With higher spike anneal temperatures at 1075°C Rs numbers as low as 1000 Ω/sq could be achieved but at the cost of Xj. At a spike

anneal temperature of 950°C, Xj ~ 12nm can be realized but at the cost of Rs numbers that is as high as 2000 Ω/sq. As a trade off at a spike anneal temperature of 1025°C, Xj ~ 15nm can be realized along with an Rs number close to 1500 Ω/sq. If we use B_{36} instead of B_{18} in the above scenario one can expect better Rs and Xj numbers.

Dimer $B_{18}H_{22}$ - 300eV, 2.33e15 atoms/cm^2 Excico Laser Anneal			
Sample	Rs	Xj at 5e18 (PCOR)	SIMS dose
	(Ohm/sq)	(nm)	(atoms/cm^2)
as-imp	x	15.2	2.33E+15
1P_1.4J/cm^2	1110	15.4	2.31E+15
5P_1.4J/cm^2	955	15.2	2.30E+15
10P_1.4J/cm^2	887	15.4	2.29E+15

Table I shows Rs and Xj data for 300eV per atom implant energy for B_{36} annealed using Excico Laser Anneal System,

Table I shows Rs and Xj data for 300eV per atom implant energy for B_{36} annealed using Excico Laser Anneal System, Basically there is no change in Xj after annealing at different number of laser pulses at a given energy density. With increasing number of pulses Rs tends to show lower values due to better activation with multiple laser pulses. Rs values less than 1000 Ω/sq can be achieved.

Fig. 7 shows boron SIMS profiles for the as-implanted and laser annealed sample for 300eV per atom implant energy for B_{36} at a dose of 2.33e15 atoms/cm^2. We did not show the SIMS profiles for 1P and 5P cases at 1.4J/cm^2 laser energy density anneals as they are identical to 10P case. There is a slight diffusion beyond the concentration lower than 1e18 atoms/cm^3. These results clearly indicate with B_{36} species one can obtain very low Xj with minimal diffusion.

Future studies will involve B_{36} species with and without cluster carbon co-implants at different implant energies for the current and future technology nodes.

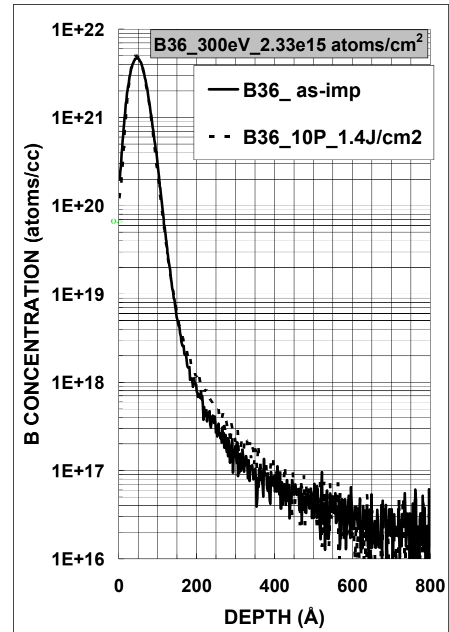

Fig. 7 shows boron SIMS profiles for the as-implanted and laser annealed sample for 300eV per atom implant energy for B_{36} at a dose of 2.3315 atoms/cm^2. We did not show the SIMS profiles for 1P and 5P cases at 1.4J/cm2 laser energy density anneals as they are identical to 10P case. There is a slight diffusion beyond the concentration lower than 1e18 atoms/cm^3.

4. Conclusions

We have shown that Cluster Ion implantation is an attractive alternative approach to realize applications in semiconductor devices at 32nm and beyond. Heavier mass of the cluster ion species like C_{16} can be substituted for both PAI and co-implant applications. For applications with ultra-low energy requirements below 500eV, B_{36} species can provide both process and throughput advantage without any device related issues due to energy contamination.

5. Acknowledgements

We thank Mattson Technology Canada and Excico Laser Inc groups for their help in annealing the wafers.

References:

[1] T. N. Horsky et al, 17th International Conf. on Ion Implantation Technology, Vol. 1066 (2008) p. 403.
[2] T. Sugii, K. Goto, T. Tanaka, J. Matsuo, I. Yamada, in: 15th International Conference on Application of Accelerators in Research and Industry, Vol. 383, (1998)
[3] K. Goto, J. Matsuo, D. Takeuchi, T. Sugii, I. Yamada, in: 14th International Conference on Application of Accelerators in Research and Industry, Vol. 937, (1996)
[4] B. J. Pawlak et al, Appl. Phys. Lett, 89 (2006) p. 062110
[5] V. Moroz et al, Appl. Phys. Lett, 87 (2005) p. 51908
[6] E. Landi, A. Armigliato, S. Solmi, R. Köghler, and E. Wieser, Appl. Phys. A **A47**, (1988) 359.
[7] S. Solmi, E. Landi, and F. Baruffaldi, J. Appl. Phys. **68**, (1990) 3250
[8]. K. Sekar et al IEEE International Conf. on Advanced Rapid Thermal Processing of Semiconductors, RTP 2007 (2007) p.
[9] J. Gelpey et al Proc. of. Electro Chem. Society (ECS) meeting (2002) p. 313
[10] W. A. Krull, B. Haslam, T. Horsky, K. Venheyden, K. Funk, Proc. 16th International Conference on Ion Implantation Technology, (2006) p. 142
[11] Maria Aboy, Lourdes Pelaz, Luis A. Marqués, Pedro López, Juan Barbolla, R. Duffy, Journal of Applied Physics, **97**, (2005) 103520